INSTITUTE OF PHYSICS PUBLISHING JOURNAL OF MICROMECHANICS AND MICROENGINEERING

J. Micromech. Microeng. **16** (2006) 1562–1570 doi:10.1088/0960-1317/16/8/017

A micro-particle positioning technique combining an ultrasonic manipulator and a microgripper

Adrian Neild[1], Stefano Oberti[1], Felix Beyeler[2], Jürg Dual[1] and Bradley J Nelson[2]

[1] Center of Mechanics, ETH Zurich, 8092 Zurich, Switzerland
[2] Institute of Robotics and Intelligent Systems, ETH Zurich, 8092 Zurich, Switzerland

E-mail: adrian.neild@imes.mavt.ethz.ch

Received 16 November 2005, in final form 19 May 2006
Published 26 June 2006
Online at stacks.iop.org/JMM/16/1562

Abstract
The acoustic radiation force acts on particles suspended in a fluid in which acoustic waves are present. It can be used to establish a force field throughout the fluid volume capable of positioning the particles in predictable locations. Here, a device is developed which positions the particles in a single line by the sequential use of two excitation frequencies which have been identified by a finite element model of the system. The device is designed such that at one end there is an opening which allows the fingers of a microgripper to enter the fluid chamber. Hence the gripper can be used to remove the last particle in the line. The high accuracy of the positioning of the particles prior to gripping means that the microgripper needs just to return to a fixed position in order to remove subsequent particles. Furthermore, the effects of the microgripper fingers entering the fluid volume whilst the ultrasound field is excited are examined. One result being the release of a particle stuck to a gripper finger. It is believed that this combination of techniques allows for considerable scope in the automation of microgripping procedures.

1. Introduction

The positioning of particles suspended in a fluid body is possible by use of the acoustic radiation force. This force is a nonlinear effect, caused by the interaction of an ultrasonic wave with a suspended particle. If second-order terms are retained when the pressure is integrated over the surface of the sphere and time averaged, then the result is the acoustic radiation force (first-order terms average over time to zero). The term 'particles' is used here to refer to any inhomogeneities within the fluid volume; this could include micro-scale solid particles, biological cells or droplets of an immiscible fluid.

Systems have been developed which are suitable for performing tasks such as filtering, particle trapping, sorting by size and aligning of particles prior to flow cytometry. Future applications are seen in micro-factories, particle handling within lab-on-a-chip devices and drug screening applications [1]. In this work a new application is explored, which is the alignment of particles prior to further handling by an external body. Here the external body is a microgripper, though it could also be, for example, a cantilever beam or a miniature suction pipette. As the particle which requires gripping is always pre-aligned between the gripper jaws, such a system is believed to allow the automation of gripping procedures. In addition, acoustic regimes to aid particle release within the fluid volume have been explored.

The majority of devices which utilize acoustic radiation forces described in the literature are acoustic filters. Such systems can partially separate two phases from each other provided that at least one is liquid or gaseous [2–4]. They operate by positioning particles in known planar locations within a flowing fluid volume using a 1D ultrasound field. By the use of carefully positioned outlets the clarified liquid between these nodal planes can be removed separately from the concentrated particle solution. These devices consist of

multiple layer resonators and when modeled are treated as 1D systems [5, 6]. One of the layers comprises of the fluid and another is the piezoelectric plate used to actuate the system. Such devices have been micromachined [7, 8], but are more usually constructed using conventional techniques. A further essentially 1D device is described by Lilliehorn *et al*, in which particles are trapped at certain locations by multiple piezoelectric elements within a fluidic system [9].

There has also been work on devices which use a macro-actuator to create a pressure field in a micromachined channel. They are capable of positioning particles in lines along the channel. At resonance these devices have what is approximately a 1D field, with the peaks and nodes occurring perpendicular to the piezoelectric plate causing the excitation. This is in direct contrast to the 1D acoustic filters in which the nodal planes are parallel to the actuator. Dougherty *et al* [10] describe a device using two coplanar transducers which are driven out of phase. Petersson *et al* [11] dispenses with the need for two out-of-phase drive signals by activating a piezoelectric plate with a single signal across the whole surface. Both devices were used to position particles in a flowing fluid volume. Such microchannel devices have been shown to be suitable for particle size separation [12]. The system developed for this work uses a piezoelectric element as an actuator, on which an active strip electrode is defined such that actuation is asymmetric. This system has been modeled to identify suitable modes using a finite element approach.

For the newly identified application of positioning particles prior to mechanical gripping, it will be necessary to position particles in a single line, in a non-flowing fluid. The particles must be close enough to an open end of the chamber that they can be reached by the gripping instrument used, and the positioning must be accurate enough that the gripper need only return to the same location for subsequent particle extraction.

2. The ultrasonic system

The application of positioning of particles prior to mechanical gripping requires a high degree of accuracy and repeatability. This accuracy is achieved by constructing the device using micromachining methods. The device, which consists of three layers, is depicted in figure 1 as (*a*) a photograph and (*b*) a cross section. The top layer is cut using a wafer saw from a glass slide. It has a thickness of 1 mm (*y*-direction as defined in figure 1), and measures 9.6 mm × 5 mm ($x \times z$). The middle layer is cut from a DRIE etched silicon wafer with a thickness of 300 μm, and measures 9.6 mm × 12 mm ($x \times z$). It has a channel etched to a depth of 200 μm. The channel itself has a width (x) of 1 mm, and length of 5 mm (y). At the end of the channel there is a circular well with the same etch depth. By placing a droplet of the particle suspension in this well the channel fills due to capillary forces. The lower layer is a piezoelectric plate measuring 9.6 mm × 5 mm ($x \times z$) with a thickness of 0.5 mm (y). This piezoelectric plate is cut in three places after being adhered to the silicon wafer. Two of the cuts can be seen in figure 1(*b*), they are to a depth of approximately 450 μm (leaving the upper electrode intact) and are made at the edges of the channel. The third cut in the piezoelectric plate is in the middle of the remaining center

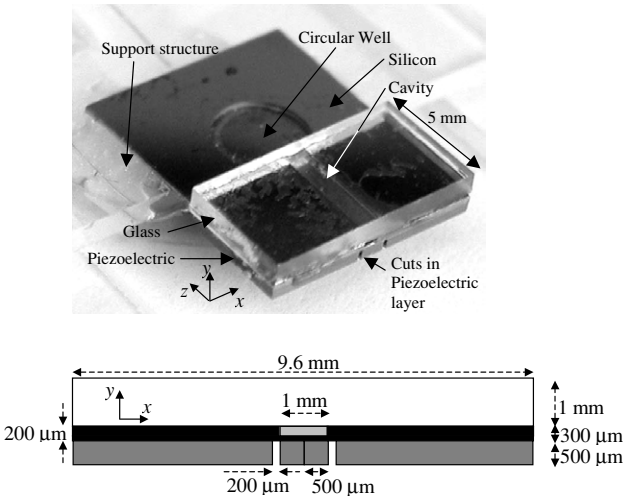

Figure 1. A photograph (*a*) and dimensioned cross-sectional depiction (*b*) of the ultrasonic positioning system.

strip of 1 mm width; the lower electrode was cut to a depth of 30 μm. This allows a voltage to be applied to just half of this strip. Hence, the actuation is asymmetric in the plane of constant x passing through the center of the fluid cavity. This is necessary as a single line of particles is desired and this requires a pressure field which is asymmetric about this plane. In operation an electrical signal is applied to an electrode on one side of this cut, all other electrodes being grounded. The piece of silicon is bonded to a support structure at the end in which the circular well is etched, the rest is left unsupported.

A finite element model of the device has been made using Femlab, a commercially available partial differential equation solver with meshing capabilities. The model is 2D and is of the cross section of the device (as in figure 1(*b*)). The boundary conditions are free displacement at all external edges, a sinusoidal voltage of a nominal 10 V on the active electrode, all other electrodes being grounded, and a fluid structure interaction between solid and fluid parts where the forces and velocities are equated. For the solid parts the governing variables are u and v, representing the displacement in the x and y directions respectively. For the fluid part the variable is pressure, p. Hence the boundary equation representing a force balance is

$$F_n/A = -n_s p \tag{1}$$

with n_s being the vector normal to the interface surface and F_n the force applied normally to the solid surface of area A. At the boundary the normal velocities are equal, this is applied to the fluid as a normal acceleration, a_n,

$$-\frac{\nabla p}{\rho_f} n_s = a_n \tag{2}$$

with ρ_f being the density of the fluid. The suspended particles are not included in the model. Damping was applied using complex stiffness parameters as given in [2]. The piezoelectric parameters used are as given by the supplier.

The result obtained from such a model is the modal shapes and the frequencies at which they occur. What is required is a prediction of how many lines will be formed. This can be found from the modal shape by the analysis of the relationship

between the pressure field and force field. The theoretical calculation of the force applied to suspended particles has been performed by Yosioka and Kawasima for the 1D case and Gor'kov for the arbitrary field case [13, 14]. Both these papers use the assumption that the particle is suspended in a large volume of fluid. In a microfluidic system the particle is always in proximity to a wall, so it can be seen that this assumption is not valid. The effect of the presence of walls is that the scattered field from the particle will be reflected. However, some points can be raised by assuming this effect does not alter the shape of the force field greatly. The pressure fields generated in the device described here are approximately 1D varying in the x-direction, for which Yosioka and Kawasima give the time averaged force as

$$\langle F \rangle = \frac{\pi r^3}{\rho_f c_f^3} P^2 \omega \sin(2kh) F_y. \tag{3}$$

The terms ρ_s and ρ_f refer to the density and c_s and c_f to the speed of sound in the particles and fluid, respectively. The particle radius is r, the angular frequency is ω, the wave number is k (given by ω/c_f), h is the distance to the nearest pressure node and P is the pressure amplitude. The term F_y is given by

$$F_y = \frac{\lambda + [2(\lambda - 1)/3]}{1 + 2\lambda} - \frac{1}{3\lambda\sigma^2}, \tag{4}$$

where $\lambda = \rho_s/\rho_f$ and $\sigma = c_s/c_f$. It can be shown that for particles which are both stiffer and denser than the fluid in which they are suspended, the term F_y is positive and therefore the particles will collect at the locations of the pressure nodes. It can be seen that for a given combination of particles and fluid the maximum acoustic radiation force is proportional to the pressure amplitude squared and the frequency. This dictates the depth of the potential well in which the particles are gathered. A second factor affecting how well lines of particles will be formed is the width of this potential well; again a higher frequency will be beneficial, as the wavelength in the fluid will decrease and with it the width of the potential well. In the consideration of (imperfect) 1D acoustic systems reference is often made to lateral forces (e.g. [2]). These much weaker forces act within the plane of the pressure node to force particles to collect at areas of acoustic radiation force potential minima.

The response of the device has been modeled over a frequency range of 0.5 to 3.0 MHz, using a 0.02 MHz frequency step. This is done by applying a harmonic voltage at each frequency in turn to the active electrode. Figure 2 shows the predicted pressure along the lower edge of the chamber for each of the frequencies examined. The graph is a grayscale in which the maximum pressure is white, the minimum is black and so the pressure nodes are gray. It is desired that a line of particles are formed along the center of the channel in preparation for further mechanical manipulation. Therefore the frequencies of interest, marked with black arrows, are 0.78 MHz and 2.14 MHz, at which 1 and 3 lines are formed respectively.

Figure 3 shows plots of the predicted vertical displacement of the solid parts of the system and the pressure within the fluid area for both the frequencies which have been identified as being of interest. Figures 3(*a*) and (*c*) show the vertical displacement at 0.78 MHz and 2.14 MHz respectively, the maximum displacements being 7.7 nm and 3.9 nm. The

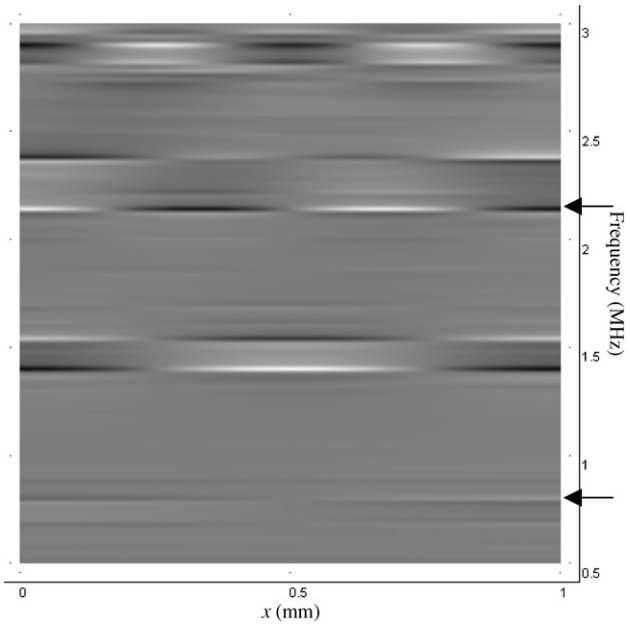

Figure 2. A grayscale plot of the pressure along the lower surface of the fluid across the width of the chamber, as a function of distance against excitation voltage frequency applied to the electrodes.

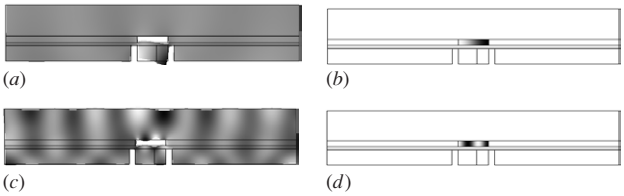

Figure 3. The predicted vertical displacement of the system at 0.78 MHz (*a*) and 2.08 MHz (*b*), and (*b*) and (*d*) the resulting pressure in the fluid chamber at the same frequencies, respectively.

grayscale plot is superimposed upon a deformed shape which is scaled in both cases by a factor of 15 000. Figures 3(*b*) and (*d*) show the pressure at the two frequencies, the maximum predicted pressure being 0.19 MPa for the case of 0.78 MHz and 1.07 MPa at 2.14 MHz. It can be seen from these plots that the pressure nodes are vertically orientated. This means that in the 3D system the nodes form vertical planes. So when the full system is viewed from above lines of particles will be seen. The particles can be expected (and indeed this has been observed experimentally) to settle to the lower surface of the fluid chamber within these vertical nodal planes. The model shows that there is no frequency at which five lines can be formed as at the frequency at which this may be expected the height of the fluid chamber starts to approach half the wavelength in the fluid, and consequently the pressure mode shapes become significantly more complicated than those shown in figures 3(*b*) and (*d*).

At 0.78 MHz the two deep cuts in the piezoelectric plate allow a large asymmetric displacement to occur in the central section of the device which is largely decoupled from the rest of the solid parts. This can be seen by a comparison of displacement amplitudes across the device. This large amplitude vibration results in the single node asymmetric

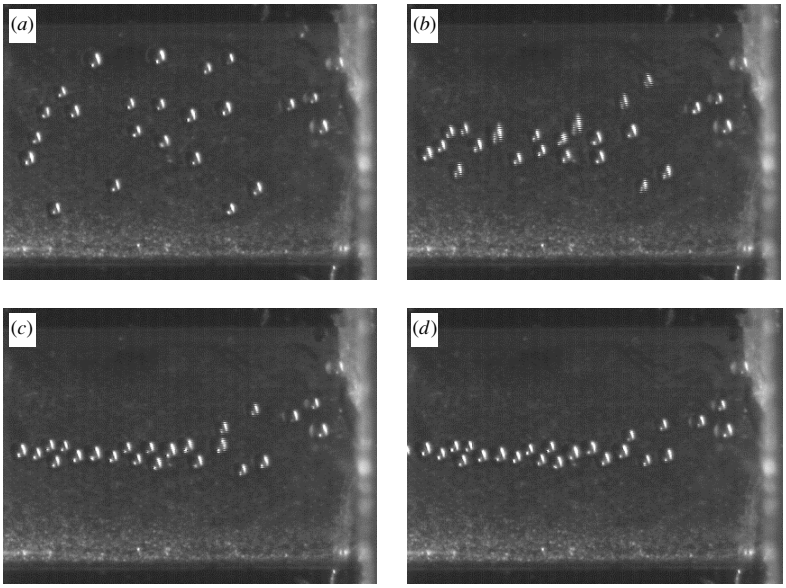

Figure 4. Line formation in the ultrasonic system by actuation at 780 kHz. The images are taken at (*a*) 0 s, (*b*) 0.2 s, (*c*) 0.4 s and (*d*) 0.6 s after the start of the excitation.

pressure field required for the application under investigation. The decoupling is much less pronounced in the resonant mode at 2.14 MHz, where the motion of the whole system is important in determining the resonant frequency. It is worth noting that if the walls which confine the fluid are considered to be rigid, and the assumption is made that in order to form one and three lines the channel must have a width of 0.5 and 1.5 wavelengths respectively, then the resonant frequencies would be predicted as 0.74 MHz and 2.22 MHz respectively. In the case of the formation of two lines, the fluid excited within rigid walls would resonate at 1.48 MHz, whilst the full finite element model predicts that two node pressure fields will occur at both 1.40 MHz and 1.54 MHz. The shifts in frequency between the simple case and the finite element model demonstrates the importance of the motion of the solid parts and so the boundary conditions at the solid/fluid interaction in the accurate determination of the resonant frequencies.

3. Results and discussions

In the experiments performed here copolymer particles (Duke Scientific) with an average diameter of 74 μm ($\pm$7%) were used. These particles were suspended in de-ionized water. In each experiment a small droplet of the solution was placed in the well at the end of the micromachined channel. The ultrasonic system was viewed from above (so the *xz* plane is seen) through a microscope (Olympus ZSH) and videos were taken with a camera (Sony CCD-IRIS, Model: SSC-M370CE) and a frame grabber (Newport, PC-IMAQ 1408). The electronic actuation was preformed using a function generator (Krone Hite, KH 3945) connected to an amplifier (ENI 2100L). The microgripper was manufactured using the process described by Sun *et al* [15]. The microgripper fingers are 2 mm long and 50 μm thick. The opening is 100 μm and it was found that a dc voltage of 90 V was sufficient to close the fingers far enough to grip the 74 μm diameter particles used. The gripper can exert a force in the order of 100 μN, as measured by a comb drive based force sensor. The microgripper was attached to a 3D positioning system (Newport, MM4006).

Figure 4 shows four images taken as the device is excited at 780 kHz using a 50 mV amplitude output from the signal generator, which causes a 21 V signal across the electrodes. The black strips at the top and bottom of the images are the walls of the channel; the separation between them is 1 mm so this gives a scale for the images. On the right-hand side, the bright line from top to bottom is the end of the device. The images are taken at (*a*) 0 s, (*b*) 0.2 s, (*c*) 0.4 s and (*d*) 0.6 s after the start of the excitation. It can be seen that a line of particles is formed along the center of the device, and that this line is much tighter away from the end of the device, indicating a drop in the maximum pressure amplitude there.

Figure 5 shows the result during actuation of the device at 2.08 MHz using a 50 mV amplitude output from the signal generator, which results in a 15.5 V signal across the electrodes. Note that the model predicted this resonance would occur at 2.14 MHz, a number of these devices were made and the best operational frequency ranged between 2.08 MHz and 2.15 MHz; this range is probably due to difference in the manufacture at the stage where the piezoelectric is glued to the rest of the system. Figure 5(*a*) shows randomly orientated particles at the end of the channel, whilst in figure 5(*b*) three lines can be seen. The interval between these two images is 0.04 s; no intermediate images can be shown as this represents the fastest possible acquisition of the camera used. Furthermore, some of the particles in the second image appear slightly elongated due to their motion whilst the shutter is open. In figure 5(*c*) a longer section of the channel is shown to give a better impression of lines which are formed.

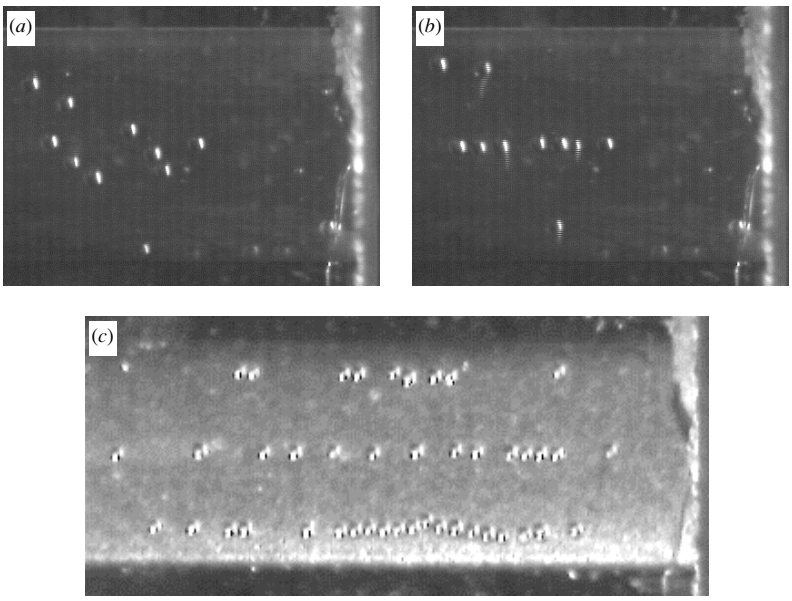

Figure 5. Line formation by actuation of the ultrasonic system at 2.08 MHz. The interval between images (*a*) and (*b*) is 0.04 s. Image (*c*) shows a longer section of the channel to give a better impression of the formation of lines.

It can be seen by examination of the two preceding experiments that both frequencies have advantages. At 780 kHz only one line is formed, consequently all the particles are accessible to the gripper, whilst at 2.08 MHz a much more accurate line is achievable. In order to obtain both advantages, the frequencies are used sequentially, firstly 780 kHz for crude gathering of the particles in the middle of the chamber and the 2.08 MHz to tighten the single line.

The goal of this work was to position particles in a line using ultrasonic forces and then to manipulate them further by use of a microgripper. Figure 6 shows a series of images from an experiment where this is achieved; three particles are successively removed from the channel and deposited on a glass slide. Again the end of the channel is clearly seen as a bright vertical line. It can be seen that the fingers of the microgripper are slightly misaligned with the channel; however the direction of motion of the positioning system is in line with the channel. The microgripper is 20 μm above (y-direction) the lower surface of the fluid chamber. Once the particle is removed from the channel it is deposited on a glass slide positioned 2 mm below the channel. The adhesive effect of the small quantity of fluid surrounding the particle causes it to stick to the substrate in preference to the microgripper; in comparison the effect of van der Waals forces is insignificant. Due to the difference in height it is necessary to refocus the microscope; hence the channel can be seen to be out of focus in figures 6(*h*), (*i*), (*l*) and (*o*). Figure 6(*a*) shows the randomly distributed particles; after excitation at 780 kHz these particles are positioned into a line along the center of the channel (figure 6(*b*)). Figure 6(*c*) shows the position of the particles after the frequency is changed to 2.08 MHz; it can be seen that the line of particles is straighter especially at the right-hand end; it is also more accurate. In the most part it is a line of single particles, where it cannot be seen that there are either two particles in contact, either next to each other or above each other (there are two bright circles which are particles in a higher layer). With a lower concentration of particles a perfect chain can be formed. In figure 6(*d*) the ultrasound has been turned off in preparation for the microgripper to enter the channel at a velocity of 0.2 mm s^{-1}. In figures 6(*e*), (*f*) and (*g*) the microgripper has been brought into position to grip the end particle, clasp it and remove it from the channel, respectively. The microgripper is then moved to the height of the glass slide, figure 6(*h*), and deposits the particle, figure 6(*i*). In order to demonstrate that this process is repeatable, an essential point in demonstrating the automation possibilities of the combination of ultrasound positioning and external gripping, the process is repeated for two further particles. The ultrasound is turned on, figures 6(*j*) and (*m*), the microgripper is brought into the chamber, figures 6(*k*) and (*n*), and the particle is successfully deposited, figures 6(*l*) and (*o*), for the second and third particles, respectively. In figure 6(*o*) the microgripper has been moved a distance of 0.5 mm to one side prior to the deposition of the particle. The accuracy of the particle alignment is such that this is the first time the microgripper needed to be moved in this direction. Due to the various stages of microgripper movement being done manually, and the need to refocus the microscope, the whole process took 270 s. However the time needed to apply the ultrasound is very small, considerably less than 1 s, while the only other major time restraint is the speed at which the microgripper can enter and exit the chamber through the fluid meniscus at the end of the channel. In this experiment it typically took 4 s for the microgripper to be moved from outside the channel to the position at which it was ready to grip the next particle, the limit at which this can be done has not been examined.

In order to further analyze the positioning accuracy of the ultrasonic system some of the images were examined using IMAQ Vision Builder. Using this software package it is possible to search for a given pattern within a given field of view for a range of images; hence it was possible to look

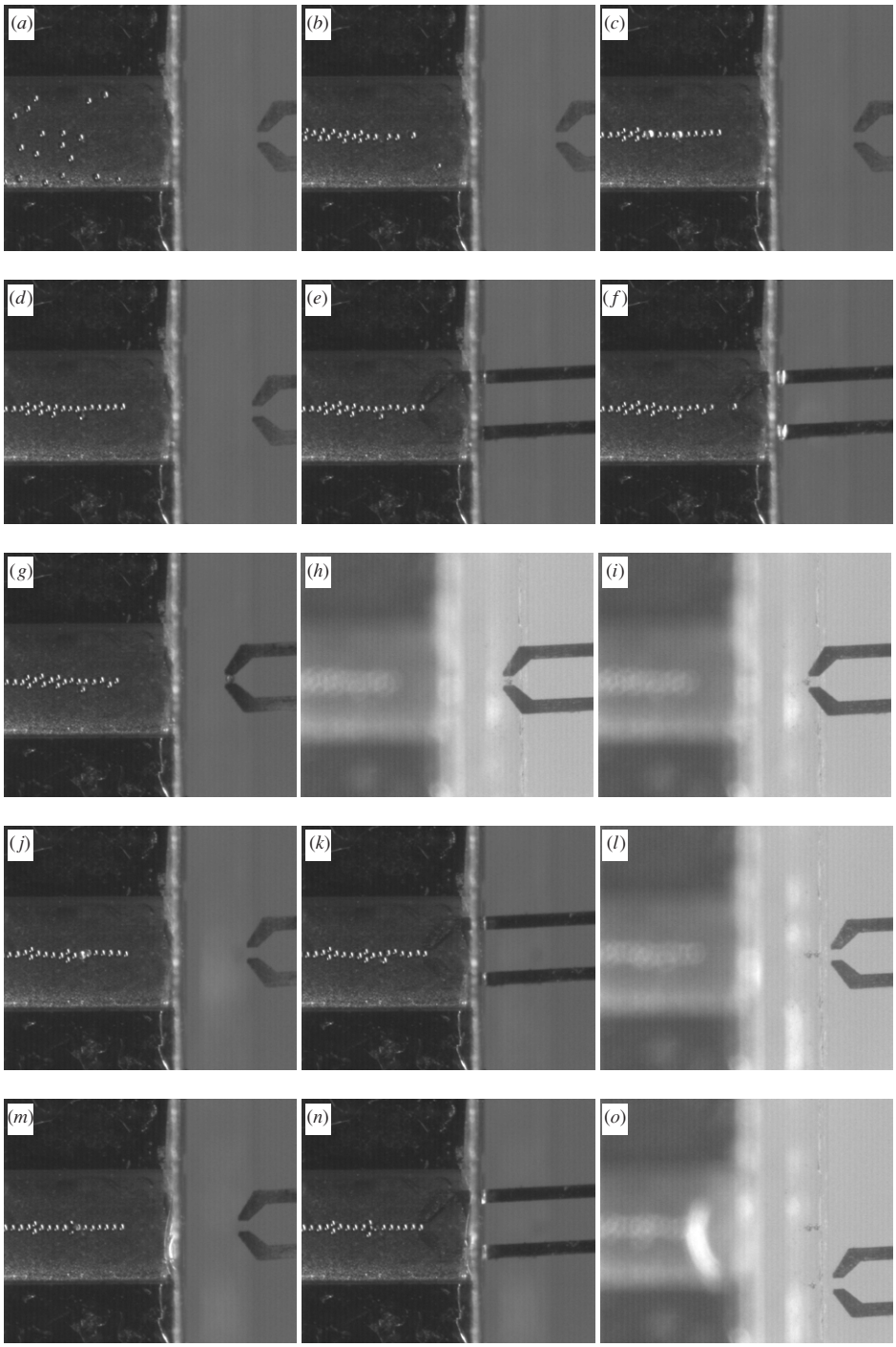

Figure 6. A series of images from an experiment in which three particles were positioned ultrasonically, gripped, removed from the channel and deposited on a glass slide, sequentially. The randomly orientated particles (*a*) are crudely aligned by excitation at 780 kHz (*b*), and then more accurately by excitation at 2.08 MHz (*c*). The ultrasound field is then turned off (*d*), in preparation for the insertion of the gripper fingers (*e*). The end particle is gripped (*f*), removed from the chamber (*g*), placed on a glass slide below the chamber (*h*) and released (*i*). The particles are then ultrasonically aligned (*j*) and (*m*), gripped (*k*) and (*n*) and released (*l*) and (*o*) for the second and third particles in the initial line respectively.

for the end particle in the line and find its position with sub-pixel accuracy. The images examined were: immediately after ultrasound was applied, after it was turned off and when the microgripper was in position to grip the particle (however prior to the gripping action being performed). This was done for each of the three particles which were handled. In the three images in which the ultrasound is on the variation in the location of the end particle was 8.8 μm. Including the images when the particles have settled after the ultrasound is turned off this figure rises slightly to 10.4 μm. Finally when all nine images are considered, the variation in the location is 14.0 μm, i.e. slightly less than the difference in the un-actuated

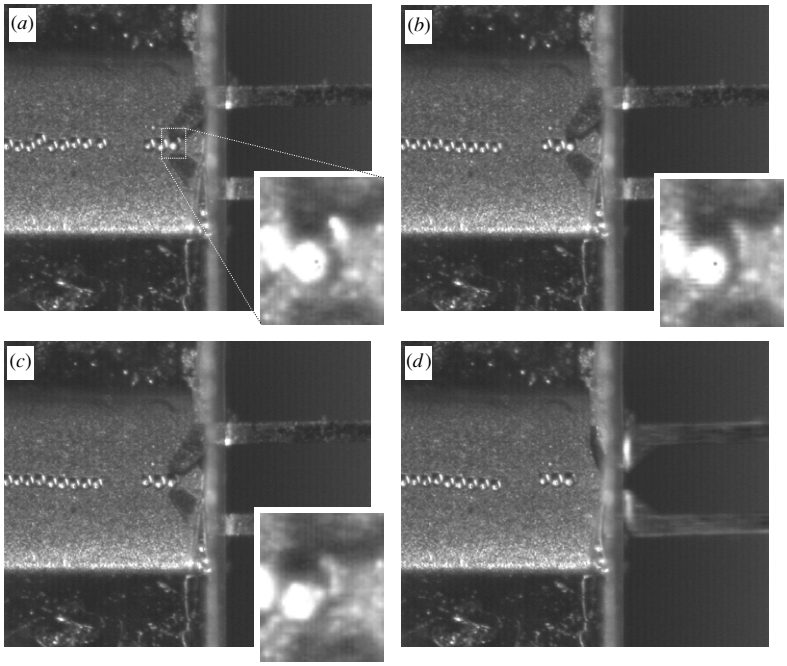

Figure 7. The release of a particle stuck on a gripper finger. Initially the particle is stuck (*a*), the ultrasound is then applied (*b*) and the particle is released (*c*). The interval between these images being 0.4 s. The insets are zoomed in images of the area shown in (*a*). The gripper can then be removed (*d*).

microgripper opening and the diameter of the particles. These three values are all for the location in the x-direction, i.e. across the channel. In the z-direction the constraints on the location are much weaker and arise due to the lateral forces which move particles to areas of minimum acoustic radiation force potential within the pressure nodal plane. The variation in the position of the end particle in the nine images was found to be 37 μm in the z-direction. It is believed that this can be further improved through altering the design of the channel.

The interaction between the microgripper and particles which occurs when the ultrasound is on whilst the microgripper is within the fluid volume has also been examined. Whilst the results are not yet as repeatable as in the case when the ultrasound is turned off prior to bringing the microgripper into the chamber, some interesting phenomena have been observed.

In figure 7 ultrasonic forces are shown to release a particle from the open microgripper. Prior to the images shown, the particles have been aligned using the two identified frequencies. Then the gripper was entered into the fluid chamber whilst the ultrasound was off and a particle gripped; in the process this particle was displaced from its original position in the upward direction (positive x) in the image. Subsequent release of the particle failed, even when the stuck particle was made to collide with the end particle left in the row; this action only caused the end two particles to adhere to the stuck particle, as can be seen in figure 7(*a*). The image shown in figure 7(*b*) appears 0.4 s later, the particle stuck to the microgripper has moved and the line of particles straightened due to excitation at 2.08 MHz. This movement is seen clearly in the change in the reflection of light from the end particle shown in the zoomed insets. Figure 7(*c*) is taken 0.4 s later, when the ultrasound is turned off, the end particle remains in its displaced position. Figure 7(*d*) shows the microgripper moved away from the released particle. Hence, ultrasonic forces have been used to aid the release of a particle from the microgripper finger. This is believed to work because, in the action of gripping, the actuated (lower) gripper finger moved the particle 10.7 μm in the x-direction. This brings it away from the location at which the minimum force potential would occur if the ultrasound were on. In the process of release the particle moves back to the original location in the x-direction to within an accuracy of just 0.2 μm.

The images shown in figure 8 are taken from an experiment in which the ultrasound was continuously on. The ultrasonic device used was different to that used in the rest of the experiments shown here and was operated at 2.15 MHz. The end of the fluid channel cannot be seen in the images, it is about 100 μm out of view to the right of the images. It is known that in this device the pressure field gets considerably weaker toward the end of the channel, to the extent that lines can no longer be formed. This is believed to be due to poor bonding between the piezoelectric layer and the underside of the silicon wafer. Figures 8(*a*) to (*c*) show the movement of the gripper to a pre-positioned particle (the images are separated by 0.2 s). In each of the images the two vertical dashed lines remain in a fixed location. As the lower finger is moved to within 100 μm of the particle, the particle is seen to move toward it and stick to it. In the last three images, figures 8(*d*), (*e*) and (*f*), the microgripper is moved rightward, so moving the adhered particle toward the exit of the chamber. It can be seen that the particle is moved from the position in figure 8(*c*) to that in figure 8(*d*) with no problem; however, as the particle is moved further (by the movement of the microgripper at a constant velocity) it becomes detached from the finger and returns through the influence of acoustic forces

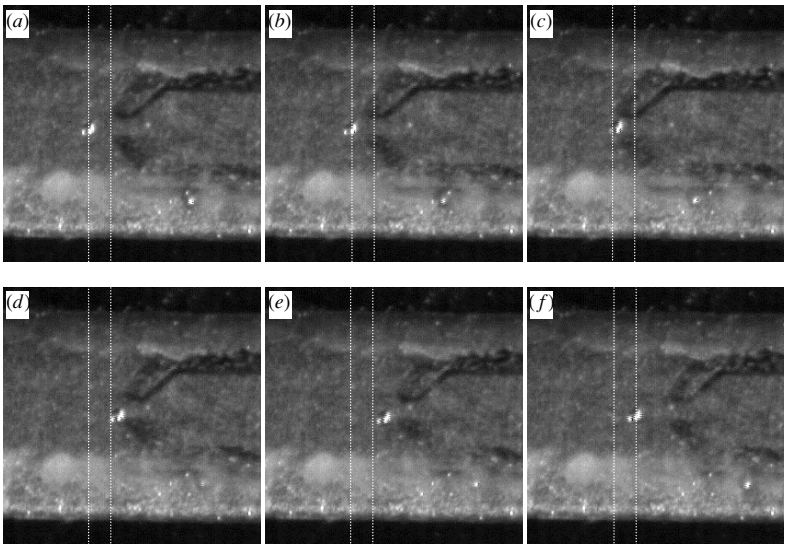

Figure 8. A series of images from an experiment in which a particle is repeatedly attached and released from a single gripper finger. The ultrasonic field was excited continuously. The gripper finger is moved toward a pre-positioned particle (*a*), the particle moves toward the gripper finger (*b*) and attaches (*c*). The images are separated by 0.2 s. The finger is then moved rightward (*d*), the particle remaining attached (*e*) and then at a repeatable location detaches and returns to its original position (*f*). Again these three images are separated by 0.2 s.

to approximately its original position (as in figure 8(*a*)). This process was repeated three times, the attachment, transport, detachment and subsequent return to original location taking place each time. The presence of secondary forces, which arise between two objects in the fluid due to ultrasound is well known (e.g. [16]). The force is attractive when both objects are stiffer and denser than the fluid. It would appear that this attractive force drops to a level lower than the primary lateral force as the particle is moved to an area in which the pressure field is known to be of lower amplitude.

4. Conclusions

Lines of particles have been formed within a fluid filled chamber using ultrasonically generated forces. The chamber has been designed so that there is open access at one end in order that the fingers of a microgripper can enter the chamber and mechanically handle the particles. It has been shown that by use of two frequencies sequentially, both identified by modeling the device, the particles can firstly be approximately positioned at the center of the chamber and then more accurately aligned. The microgripper has been used to successfully remove the end particle from the chamber and deposit it on a glass slide; this was done repeatedly without the need to move the gripper in the direction perpendicular to the line of particles, such was the accuracy with which they could be aligned.

Further experiments were carried out to investigate the effect of the ultrasonic vibration of the fluid whilst the microgripper fingers were within the chamber. It was found that the release of a particle stuck to one finger of the microgripper was possible by brief ultrasonic actuation. In addition a particle has been shown to be attached to and released from a single gripper finger through the continual use of ultrasound.

It is believed that the combination of such an ultrasonic actuator and mechanical gripper has many applications. Firstly it has been shown that in order to collect subsequent particles the microgripper need only return to one position, so allowing the automation of the gripping system, either for sequential handling using one gripper, or simultaneous handling using an array of grippers and equivalently spaced particle lines. Such well-defined spacing of lines would be possible in either numerous single line forming chambers or numerous lines in one chamber. This setup would also allow particles to be collected from one line, and after an intervening action deposited in another line using ultrasonic release as has been demonstrated. In addition it is believed that such a system is not restricted to the handling of inert particles; it would also be possible to handle, for example, biological cells, which could lead to applications in biotechnology.

Acknowledgments

This work was supported by KTI/CTI, Switzerland, through a Top Nano 21 grant, project numbers 6643.1 and 6989.1.

References

[1] Haake A, Neild A, Radziwill G and Dual J 2005 Positioning, displacement, and localization of cells using ultrasonic forces *Biotechnol. Bioeng.* **92** 8–14
[2] Gröschl M 1998 Ultrasonic separation of suspended particles: Part I. Fundamentals *Acustica* **84** 432–47
[3] Gröschl M, Burger W and Handl B 1998 Ultrasonic separation of suspended particles : Part III. Application in biotechnology. *Acustica* **84** 815–22
[4] Benes E, Burger W, Groeschl M and Trampler F 1995 Method for treating a liquid *Patent EP* 0 633 049 A1; (1995-01-11)
[5] Hill M, Shen Y and Hawkes J J 2002 Modeling of layered resonators for ultrasonic separation *Ultrasonics* **40** 385–92

[6] Nowotny H and Benes E 1987 General one-dimensional treatment of the layered piezoelectric resonator with two electrodes *J. Acoust. Soc. Am.* **82** 513–21
[7] Harris N R, Hill M, Beeby S, Shen Y, White N M, Hawkes J J and Coakley W T 2003 A silicon microfluidic ultrasonic separator *Sensors Actuators* B **95** 425–34
[8] Harris N, Hill M, Shen Y, Townsend R J, Beeby S and White N M 2004 A dual frequency, ultrasonic, microengineered particle manipulator *Ultrasonics* **42** 139–44
[9] Lilliehorn T, Nilsson M, Simu U, Johansson S, Almqvist M, Nilsson J and Laurell T 2005 Dynamic arraying of microbeads for bioassays in microfluidic channels *Sensors Actuators* B **106** 851–8
[10] Dougherty G M and Pisano A P 2003 Ultrasonic particle manipulation in microchannels using phased co-planar transducers *Proc. 12th Int. Conf. on Solid State Sensors, Actuators and Microsystems (Boston)* pp 670–3
[11] Petersson F, Nilsson A, Holm C, Jönsson H and Laurell T 2005 Continuous separation of lipid particles from erythrocytes by means of laminar flow and acoustic standing wave forces *Lab on a Chip* **5** 20–2
[12] Kapishnikov S, Kantsler V and Steinberg V 2006 Continuous particle size separation and size sorting using ultrasound in a microchannel *J. Stat. Mech.* P01012
[13] Yosioka K and Kawasima Y 1955 Acoustic radiation pressure on a compressible sphere *Acustica* **5** 167–73
[14] Gor'kov L P 1961 Forces acting on a small particle in an acoustic field within an ideal fluid *Dokl. Akad. Nauk Sssr* **140** 88–92
[15] Sun Y, Potasek D P, Bell D J, Fry S N and Nelson B J 2005 Characterizing fruit fly flight behavior using a microforce sensor with a novel comb drive configuration *IEEE/ASME J. Microelectromech. Syst. (JMEMS)* **14** 4–11
[16] Weiser M A H, Apfel R E and Neppiras E A 1984 Interparticle forces on red cells in a standing wave field *Acustica* **56** 114–9